New superconducting scanning phonon spectroscopy

I. Iguchi, Y. Kasai, and Y. Suzuki*
Institute of Materials Science, University of Tsukuba, Sakura-mura, Ibaraki 305, Japan
(Received 17 October 1985; revised manuscript received 31 December 1985)

A new phonon-detection technique utilizing superconducting tunnel junctions is introduced. In this technique the high-frequency phonons emitted from a generator are detected by a superconducting sensor placed apart from it by a thin layer ($\lesssim 100$ μm) of liquid helium. The sensor is either a single-tunnel junction or a double-tunnel junction. The phonon signal increases nonlinearly with an increase of generator current. In the case that a double-tunnel-junction sensor is used, the information on the energy spectrum of the transmitted phonons is obtained by varying the detectable phonon cutoff energy by quasiparticle injection. For the phonons emitted from a superconducting tunnel junction, a clear change at the phonon cutoff energy equal to the generator gap is observed. The spatial scanning spectroscopy with a spatial resolution of 20 μm is performed by moving a sensor relative to the generator. The observed phonon spatial distribution has a periodically modulated structure for the superconducting tunnel generator accompanying a diffusive instability. The limits and applications of this technique are also discussed.

I. INTRODUCTION

The emission and detection of high-frequency phonons utilizing superconducting tunnel junctions has been going on for many years.[1] In most of these experiments, a generator and a detector are mounted on the two opposing surfaces of a single crystal such as sapphire or germanium. The phonons emitted from the generator pass through the single crystal and are detected by a superconducting tunnel detector. With this spectroscopy, two types of methods of obtaining information on the phonons were developed. One was time-of-flight measurement, and the other was dc measurement with changing generator current. Both measured important properties of phonons in nonequilibrium superconductors. For the measurement of the phonon energy distribution, stress-tunable phonon spectroscopy was developed, which enabled us to study the 2Δ-phonon emission from a superconducting tunnel junction[2] and from a Josephson junction.[3]

In this paper, we introduce a new phonon spectroscopy technique different from the above method. In our method, the phonons emitted from a generator are detected by a superconducting tunnel junction separated from it by a thin layer of liquid helium. Several features of this method are stated as follows: (i) The spatial distribution of the emitted phonons is measurable since a generator and a detector may be mounted on different sample stages which are independently movable. In fact, we have already reported the measurement of the spatial distribution of phonons from the multiple-gap states of nonequilibrium superconductors, due to a quasiparticle-injection-induced instability.[4,5] (ii) The detection efficiency of the emitted phonon power is high when the generator-detector separation is made small (<100 μm) due to small attenuation of phonons in liquid helium. (iii) The spectroscopic study of incident phonons on a detector (or sensor) may be performed using a gap-tunable phonon sensor by quasiparticle injection. In this case, the sensor is made of a double-tunnel-junction structure in which one junction serves as an injector of quasiparticles into a middle film. This method applies to the detection of phonons not only from superconductors but also from metals or semiconductors in the nonequilibrium state.

In Sec. II, the principle of phonon detection is described, and in Sec. III, we calculate the phonon-sensor sensitivity. The experimental arrangement is described in Sec. IV, and Sec. V is devoted to the experimental results and discussions. Section VI finally states the advantages of this phonon spectroscopy and its future aspects.

II. PRINCIPLE OF PHONON DETECTION

Figure 1 illustrates the principle of phonon detection. Physically, the emitted phonons from a generator passing through the film-helium boundary propagate with some attenuation or are completely converted to other excitations in the superfluid helium due to collisions with the excitations present. In any case, the excitations which reach the surface of a sensor film again interact with the helium-film boundary and are injected into a sensor film.

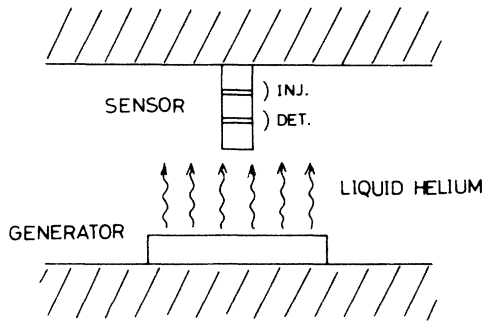

FIG. 1. Principle of phonon detection. The phonon sensor can be a single- or a double-tunnel junction.

Those phonons with energy greater than the sensor gap are capable of pair breaking in a film, and the corresponding signal is detected by the sensor junction. As a phonon sensor, we use a *S-I-S* or a *S-I-N* junction (*S*: superconductor, *N*: normal metal, *I*: insulator) for the phonon intensity measurement and a *S-I-S-I-S* or a *S-I-S-I-N* double-tunnel junction for obtaining the spectral information. The sensor gap is equal to its thermal equilibrium value $2\Delta_{eq}$ in the case of no injection from an adjacent injector and is equal to the nonequilibrium value $2\Delta_s^*$ in the case of injection. Hence, for phonon spectroscopic study, sensor films are exposed to dual injection of quasiparticles and phonons from an adjacent injector and a generator. The signal from an injector is generally much greater than that from a generator.

Suppose that the nonequilibrium phonon distribution in a generator film is given by $n(\omega)$. Then the phonons emitted from the generator in the frequency range $(\omega,\omega+d\omega)$ per unit time become proportional to

$$\frac{n(\omega)-n(\omega,T)}{\tau_{es,g}}\omega^2 d\omega \ , \tag{1}$$

where $n(\omega,T)$ is the thermal equilibrium phonon distribution at an ambient temperature T. We have assumed that the phonon density of states is proportional to ω^2. $\tau_{es,g}$ is the phonon escape time of generator films, approximately given by $4d/\eta c_s$, where d is the total film thickness, c_s is the sound velocity, and η is the average phonon transmission probability through the film-helium boundary. In this approximation, the effect of Kapitza boundary resistance is simply included in the factor η. If the film surface is smooth, the direction of the emitted phonons at the initial stage is confined within a narrow cone determined by the critical angle $\theta_c \simeq 5°$, since the sound velocity in superconductors is much greater than that in liquid helium.[6]

On the other hand, if a sensor film is exposed to a phonon injection rate of I_{ph}, the increase in the quasiparticle number density in the steady state is calculated using the Rothwarf-Taylor equations[7] to give

$$\delta N^* = \left[N^{*2} + \frac{I_{ph}\tau_{es,s}}{R\tau_B} \right]^{1/2} - N^*$$

$$\simeq \frac{I_{ph}\tau_{es,s}}{2RN^*\tau_B} \quad \text{for} \quad \delta N^* \ll N^* \ , \tag{2}$$

where N^* is the steady-state quasiparticle number density by injection from an adjacent injector only, R is the quasiparticle recombination coefficient, τ_B is the phonon pair-breaking time, and $\tau_{es,s}$ is the phonon escape time of sensor films. Assuming the linear relation $\delta\Delta^* = -\delta N^*/2N(0)$, where $N(0)$ is the single spin density of states at a Fermi level, we obtain

$$\delta\Delta_s^* = S^* I_{ph}, \quad S^* \equiv \frac{\tau_{es,s}\tau_R}{2N(0)\tau_B} \ , \tag{3}$$

where $\tau_R = 1/(2RN^*)$ is the quasiparticle recombination time in the nonequilibrium state. When the sensor film is in the thermal equilibrium state ($\Delta_s^* = \Delta_{eq}$), Δ_s^*, τ_R, and τ_B in (3) should be replaced by Δ_{eq}, τ_{RT}, and τ_{BT}, the quantities in the thermal equilibrium, respectively. Then S^* is replaced by its thermal value S,

$$S \equiv \frac{\tau_{es,s}\tau_{RT}}{2N(0)\tau_{BT}} \ . \tag{4}$$

The factors S^* and S are determined by the quantities only characteristic of a sensor film; hence, they represent the sensor sensitivity when the gap is directly measured.

As for the nature of transmitted excitations, it is possible to conjecture second sound or ballistic ultrahigh-frequency phonons or other types of excitations. In our experimental temperature range ($1.3\ \text{K} \leq T \leq 2.0\ \text{K}$), however, it is natural to consider second sound since the phonons are expected to interact very strongly with the excitations such as phonons or rotons in superfluid helium. The nonequilibrium phonons in a generator are produced by dc transport current in this experiment. Hence, second sound of low frequency and large amplitude would be expected.

Suppose that the transmitted excitations would be second sound. Because of the thermal nature of excitations, the original phonon spectral shape would be completely lost and the detected phonon spectrum would show a simple Planck distribution. For the measurement of phonon intensity from a generator, this matter causes almost no problem, since the integrated energy flux is measured. For the measurement of the spatial distribution of phonons, it will also give a sensible result, provided that the separation between the generator and the sensor is made comparable to or smaller than the spatial scale of the inhomogeneous distribution. For the spectroscopic measurement, as stated above, only the information on the incoming temperature wave will be obtained. As shown later, however, the experimental data showed a significant deviation from the thermal spectrum in the case where a superconducting tunnel junction was used as a generator. This means that the spectral information of a generator is still kept, to some extent, for some other reasons. This may be attributed to the special situation, where second sound was confined to the narrow-gap region in our experiment, or to the partial involvement of the excitations different from second sound, such as ultrahigh-frequency ballistic phonons (e.g., 2Δ phonons in tin have an energy of 13 K comparable to the maximum energy in the spectrum of the elementary excitations in liquid helium) or other types of excitations. Unfortunately, it is quite difficult to perform the time-of-flight measurement in our experimental arrangement to determine the nature of excitations due to the cross-talk problem.

III. CALCULATION OF SENSOR SENSITIVITY AND PHONON SIGNAL

For an *S-I-S* junction, there are two methods for detecting the phonon signal, as illustrated in Fig. 2. One method is to detect an increase in the quasiparticle current, the other is to detect the gap reduction directly at the current-rise portion of the *I-V* characteristic curve. It is clear that the former method has a much higher sensitivity than the latter. The latter method provides, however, a simple analysis for the spectroscopic measurement

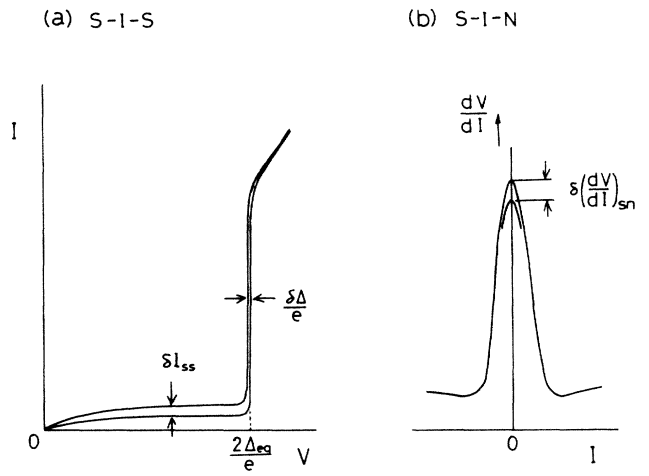

FIG. 2. Response of a sensor junction to incident phonons: (a) S-I-S junction, (b) S-I-N junction.

because of direct detection of the gap value itself.

In the following discussion, we consider the case in which the sensor films are in the thermal equilibrium state. The tunnel current for an S-I-S junction is given by

$$I_{ss}=AN_1(0)N_2(0)\int_{-\infty}^{\infty}\rho_1(E)\rho_2(E+eV)\times[f(E)-f(E+eV)]dE\ , \tag{5}$$

where V is the bias voltage of a sensor-detector junction and $f(E)$ is the quasiparticle distribution function. $\rho(E)=|E|/(E^2-\Delta_{eq}^2)^{1/2}$ is the BCS density of states and the subscripts 1 and 2 refer to two superconducting films of a junction. A is proportional to the tunneling probability and is connected to the normal conductance by the relation $G_n=AN_1(0)N_2(0)$. The increase in the quasiparticle current due to the phonon injection rate I_{ph} is calculated from Eq. (5), which, for $\Delta_{eq}/k_BT\gg1$, is approximately given by

$$\delta I_{ss}\simeq G_n g(V)SI_{ph}/e\ ,\qquad g(V)\equiv\frac{eV+\Delta_{eq}}{[eV(eV+2\Delta_{eq})]^{1/2}}\ , \tag{6}$$

where we used the relation $\delta N^*=2N(0)SI_{ph}$. Then the phonon signal in terms of the voltage change is obtained as

$$\delta V\simeq G_n\left[\frac{dV}{dI}\right]_{ss}g(V)SI_{ph}\ , \tag{7}$$

where $(dV/dI)_{ss}$ is the differential resistance in the superconducting state. $g(V)$ is weakly dependent on V for $\Delta_{eq}/e\lesssim V\lesssim 2\Delta_{eq}/e$ and roughly equal to 1.

In the case where the gap change is directly measured, we have

$$|\delta\Delta_s^*|=SI_{ph}\ . \tag{8}$$

A comparison between Eqs. (7) and (8) shows that the measurement of δV has a better sensitivity than that of $\delta\Delta_s^*$ by a factor of $G_n(dV/dI)_{ss}$, which is proportional to

$$(\Delta_{eq}/k_BT)^{1/2}\exp(\Delta_{eq}/k_BT)$$

and becomes considerably greater as the bath temperature is reduced. For example, it becomes about 26 times greater in going from $T=1.8$ to 1.0 K.

On the other hand, in the case of an S-I-N junction, the phonon signal is detected as the change in the differential resistance at zero bias voltage (see Fig. 2), which is calculated from the tunneling formula and Eq. (8). When $\Delta_{eq}/k_BT\gg1$, it becomes

$$\delta\left[\frac{dV}{dI}\right]_{sn}\simeq G_n^{-1}(2\pi\Delta_{eq}k_BT)^{-1/2}\exp(\Delta_{eq}/k_BT)SI_{ph}\ . \tag{9}$$

Equations (7)—(9) also hold for the case where sensor films are in the nonequilibrium state by quasiparticle injection from an adjacent injector if we replace T, Δ_{eq}, and S by T^*, Δ_s^*, and S^*, where T^* is some effective temperature. The condition $\Delta_s^*/k_BT^*\gg1$, however, does not hold when Δ_s^* is significantly smaller than Δ_{eq}; in that case, the analysis of δV or $\delta(dV/dI)_{sn}$ becomes complicated. In this sense, the direct measurement on $\delta\Delta_s^*$ is not affected by the above condition and provides simple information.

Now we discuss how the S^* or S factors are calculated theoretically. Since the S^* and S factors depend on the quasiparticle recombination time and the phonon pair-breaking time, which are generally dependent on energy, distribution function, and bath temperature; in order to be adapted to the energy-independent rate equations, we introduce the average value of the quasiparticle and phonon lifetimes over energy as follows:

$$\langle\tau_R\rangle^{-1}\equiv\int_{\Delta_s^*}^{\infty}\tau_R(E)^{-1}f_s(E)\rho(E)dE\Big/\int_{\Delta_s^*}^{\infty}f_s(E)\rho(E)dE\ , \tag{10}$$

$$\langle\tau_B\rangle^{-1}\equiv\int_{2\Delta_s^*}^{\infty}\tau_B(\omega)^{-1}n_s(\omega)\omega^2d\omega\Big/\int_{2\Delta_s^*}^{\infty}n_s(\omega)\omega^2d\omega\ , \tag{11}$$

where $f_s(E)$ and $n_s(\omega)$ are the nonequilibrium quasiparticle and phonon distribution functions of a sensor film, respectively. Then S^* is given by

$$S^*=\frac{\tau_{es,s}\langle\tau_R\rangle}{2N(0)\langle\tau_B\rangle}\ , \tag{12}$$

where the phonon escape time was assumed to be independent of energy. The average lifetimes $\langle\tau_R\rangle$ and $\langle\tau_B\rangle$ have been very recently calculated[8] in the cases of the μ^* and T^* models.[9,10] In Fig. 3, we show the calculated results of $2N(0)\tau_{es,s}S^*=\langle\tau_R\rangle/\langle\tau_B\rangle$ as a function of the nonequilibrium gap parameter Δ_s^*. When $\Delta_s^*=\Delta_{eq}$, it gives the S value. The function first decreases very rapidly with an increase of quasiparticle injection owing to rapid shortening of the quasiparticle recombination time, then decreases slowly. It is surprising that the behaviors for the μ^* and T^* models are almost the same, although these two models are based on opposite physical situations ($\tau_{es,s}/\langle\tau_B\rangle\ll1$ and $\tau_{es,s}/\langle\tau_B\rangle\gg1$) from each other.

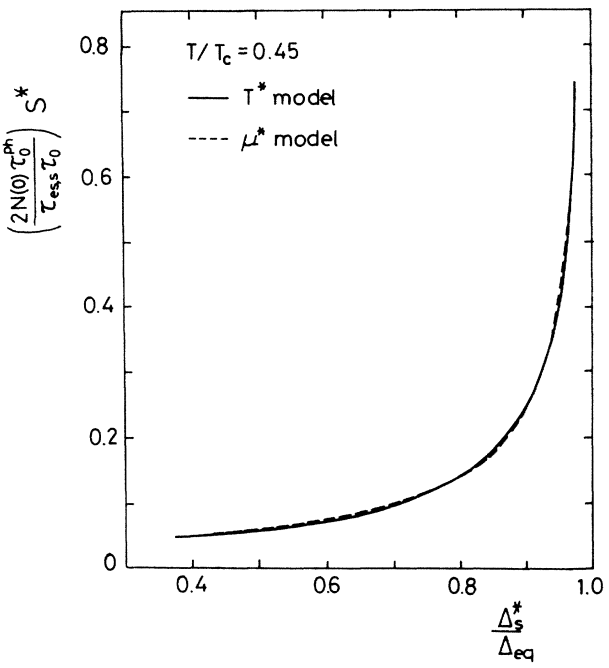

FIG. 3. Sensor sensitivity factor as a function of normalized nonequilibrium gap parameter Δ_s^*/Δ_{eq} for the T^* and μ^* models.

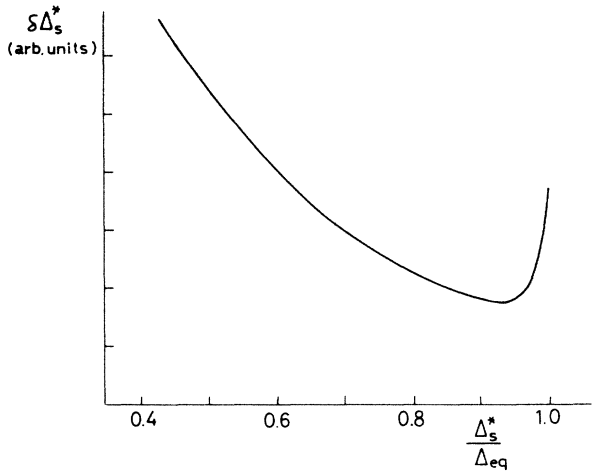

FIG. 4. Calculated phonon signal in terms of sensor gap reduction as a function of the normalized sensor gap parameter Δ_s^*/Δ_{eq} at $T/T_c=0.44$ when the generator effective temperature is $T^*/T_c=0.47$. Note that, for the calculation, the experimental S^* factor (Fig. 7) was assumed.

Next we discuss how the S^* factor is related to the experimentally measurable quantities. This is important since it provides more real information on S^*. First we obtain the curve for Δ_s^* versus the injected power P, using quasiparticle injection from a sensor injector only, from which the relation between $d\Delta_s^*/dP$ and Δ_s^* is obtained. Now, if there were an extra phonon power injection P' from a generator in addition to quasiparticle injection, the expected gap decrease $\delta\Delta_s^*$ would be nearly equal to $(d\Delta_s^*/dP)P'$. On the other hand, we have the relationship $\delta\Delta_s^*=S^*I_{ph}$; hence,

$$S^*=(d\Delta_s^*/dP)P'/I_{ph} .$$

P' is approximately equal to $2\Delta_s^*I_{ph}$ and finally we obtain $S^*\simeq 2\Delta_s^*(d\Delta_s^*/dP)$, where the quantities on the right-hand side are obtained purely experimentally.

Using the S^* factor obtained above, we now try to calculate the expected phonon signal in terms of gap reduction in a sensor film as a function of the sensor nonequilibrium gap parameter Δ_s^*. When a generator is a current-carrying homogeneous metal film, the simple heating spectrum is expected. This situation will not be changed by propagation of the emitted phonons in terms of second sound in superfluid helium. In this case, from Eq. (1), I_{ph} becomes proportional to the following quantity:

$$I_{ph}\propto\Gamma\int_{2\Delta_s^*}^{\infty}\frac{n(\omega,T^*)-n(\omega,T)}{\tau_{es,g}}\omega^2 d\omega , \qquad (13)$$

where Γ is the second-sound attenuation factor and $n(\omega,T^*)$ is the phonon distribution function at the effective temperature T^*. In Fig. 4, we show a calculated result when the sensor is a tin junction ($2\Delta_{eq}=1.15$ meV) and $T^*=1.75$ K and $T=1.65$ K. This applies to the case where a thin NiCr film heater is used. The rapid decrease just below $\Delta_s^*/\Delta_{eq}=1$ is simply due to the rapid shortening of the quasiparticle recombination time by quasiparticle injection in the S^* factor.

We also mention, that when a superconducting junction is used as a generator and the original $2\Delta_g^*$-phonon spectrum shape is assumed to be kept during propagation, the calculation shows a slope discontinuity at $\Delta_s^*=\Delta_g^*$.

IV. EXPERIMENTAL

A phonon generator and a sensor were mounted on different sample stages which were independently movable. These sample stages were controllable by a special gear system, as illustrated in Fig. 5. One stage was movable along the x and y axes and the other along the z axis, with a spatial resolution of 20 μm, using the micrometers attached outside the cryostat. The generator-sensor distance was kept at 50—150 μm in order to obtain an appreciable signal. Special care was taken in attaching the current and voltage leads to the substrate, using silver paste. The generator-sensor distance was measured by projecting light on the strip line of the upper substrate with a given angle and observing its shadow on the lower substrate.

As for a sensor, we used several types of junctions: S-I-S (S:Sn), S-I-S' (S:Sn, S':Pb), S-I-N (S:Sn, Pb, In; N: Cu coated with a thin NiCr film), S-I-S-I-S (S:Sn), and S-I-S-I-N (S:Sn; N: Cu coated with a thin NiCr film). The junctions were fabricated by subsequent evaporation and oxidation of films utilizing a set of metal masks at room temperature. The film thicknesses were 2000—3000 Å and the junction size ranged from 20×20 to 300×500 μm^2.

As a generator, we used Sn-I-Sn and Sn-I-Sn-I-Sn junctions for studying the phonons from nonequilibrium su-

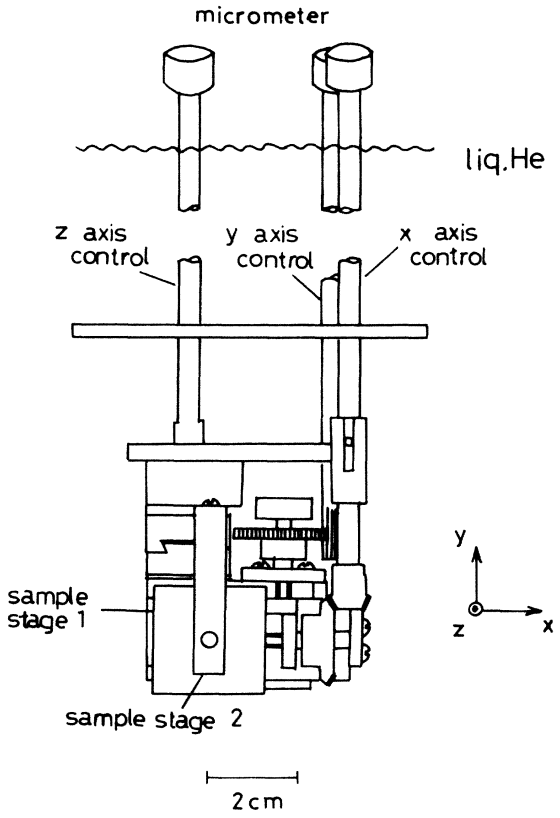

FIG. 5. Schematic drawing of the driving system of the sample stages along the x, y, and z directions.

perconductors. For the double-tunnel-junction sample, one junction was a phonon generator and the other junction served as a detector to check the superconducting properties in the nonequilibrium state under quasiparticle injection. For the detection of phonons from metal films, we used a thin NiCr film of a few hundred Å. The size of a generator was 0.3—1.0 mm, always greater than the size of a sensor used.

One might ask whether the phonons emitted from the sensor injector could disturb the nonequilibrium state produced by quasiparticle injection of a generator, but it was confirmed that their effect caused gap reduction less than a few microvolts in the case of superconductors, hence giving a negligible effect as compared with the gap reduction of several hundred microvolts caused by a generator current.

V. RESULTS AND DISCUSSION

A. Sensor junction characteristics

Figure 6 shows the behavior of the sensor gap reduction when increasing the power density P injected into a sensor-injector junction at $T=1.6$ K for a Sn-I-Sn-I-Sn double-tunnel-junction sensor. The derivative $d\Delta_s^*/dP$ versus P curve is also shown. The detector I-V characteristics under injection were sufficiently sharp down to ~ 0.55 mV but they smeared rapidly thereafter, indicating a loss of sensitivity. Therefore, for phonon spectroscopy,

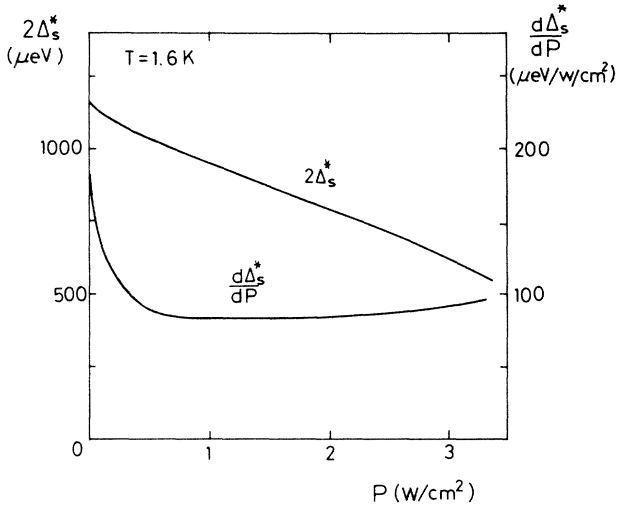

FIG. 6. Typical behavior of sensor gap reduction against the injected power density P for a double-tunnel-junction sensor. The derivative of this curve ($d\Delta_s^*/dP$) is also shown.

such analysis may be possible for the energy range ($2\Delta_{eq}, \sim\Delta_{eq}$). Figure 6 shows that Δ_s^* decreases roughly linearly with P, but the deviation from linearity is clear, indicating that the quasiparticle-injected state is not a simple heating state.[11]

The average sensor sensitivity is about 90 μeV/W/cm^2. This gives that the gap reduction of 0.1 μeV corresponds to the input power density of 600 μW/cm^2. This efficient gap reduction comes from the high phonon trapping factor for tin films (about 20). If the response is measured in terms of the voltage change in the excess current part, the sensitivity is increased by about an order of magnitude at $T=1.6$ K. By reducing the bath temperature, it is increased by another order of magnitude. Hence the sensor junction enables us to detect the input power density of a

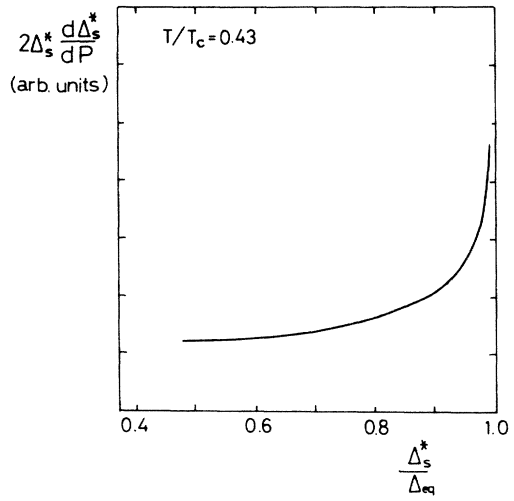

FIG. 7. Calculated curve of $2\Delta_s^*(d\Delta_s^*/dP) \simeq S^*$ as opposed to the normalized nonequilibrium gap parameter Δ_s^*/Δ_{eq}, based on the data in Fig. 6.

few $\mu W/cm^2$.

Figure 7 shows the quantity $2\Delta_s^*(d\Delta_s^*/dP) \simeq S^*$ calculated from Fig. 6 as a function of Δ_s^*/Δ_{eq}. The qualitative behavior is similar to the theoretical curve of S^* (Fig. 3), but the experiment showed a more steeply decreasing behavior for $\Delta_s^*/\Delta_{eq} > 0.9$ and a more gradually decreasing behavior for $\Delta_s^*/\Delta_{eq} < 0.9$.

B. Phonon signal through liquid helium

The detected maximum phonon signal in terms of power density when $\Delta_s^* = \Delta_{eq}$ almost corresponded to 1% of the injected power density into a generator, and generally it ranged from 10^{-2} to 10^{-3}. This ratio increased by several factors when Δ_s^* becomes significantly less than Δ_{eq}.

Figure 8 shows the phonon signal in terms of gap reduction as a function of generator current detected by a Sn-*I*-Sn-*I*-Sn double-tunnel-junction sensor placed 80 μm away from a thin NiCr film heater of a few hundred Å and $R \simeq 5\Omega$. The dissipated power of the NiCr heater at $I_g = 30$ mA was 4.5 mW corresponding to the power density of $3 W/cm^2$. The sensor gap was biased at three different values $2\Delta_s^* = 1.15 (= 2\Delta_{eq})$, 1.00, and 0.520 meV by quasiparticle injection from the sensor-injector junction. All curves exhibited qualitatively similar behavior. The detected phonon signal was very small for smaller generator current but increased rapidly for larger current. The calculated results based on the simple heating model showed qualitatively similar behavior. We mention that

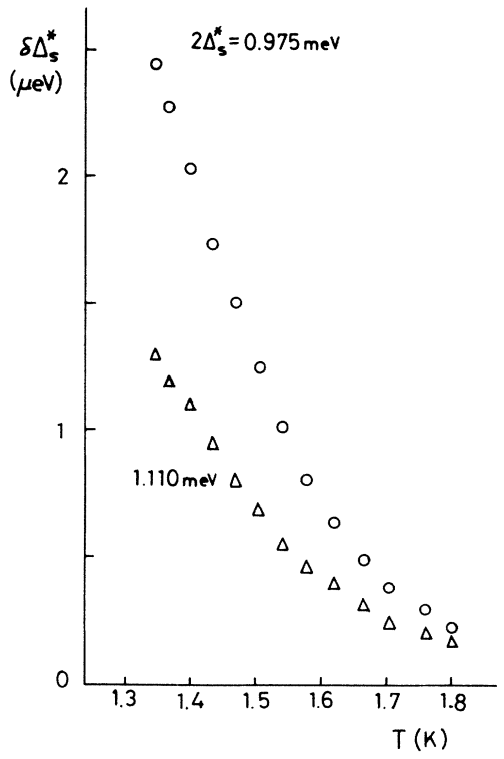

FIG. 9. Temperature dependence of the detected phonon signal in terms of sensor gap reduction for two different sensor cutoff energies.

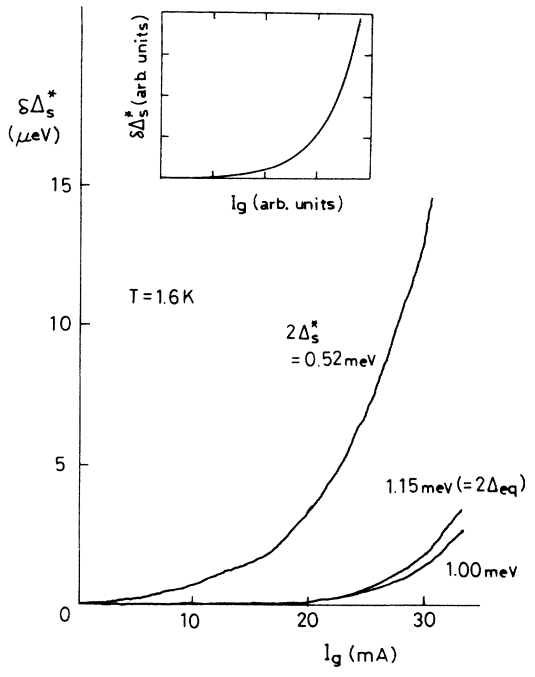

FIG. 8. Dependence of the detected phonon signal in terms of sensor gap reduction on generator current when the sensor gap is 1.15 ($=2\Delta_{eq}$), 1.00, and 0.520 meV. The inset shows the calculated result based on Eqs. (3) and (13) for the case of $2\Delta_s^* = 1.00$ meV.

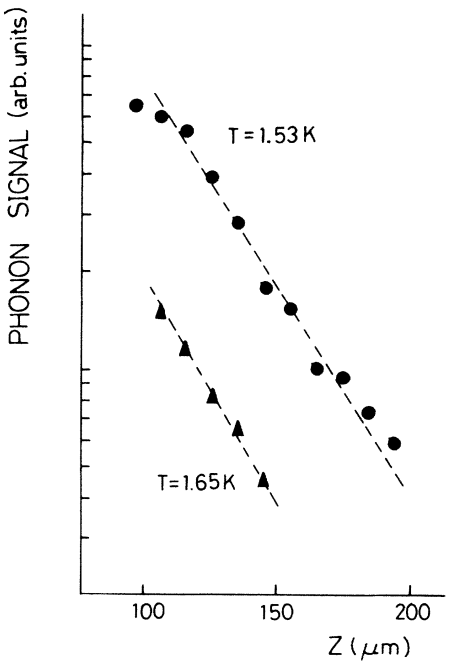

FIG. 10. Dependence of the detected phonon signal on the generator-sensor distance z at two different bath temperatures.

the phonon signal increased nonlinearly even against the power. In the case of use of a superconducting junction as a generator, the phenomena were found to be qualitatively the same.

Figure 9 shows the temperature dependence of the detected phonon signal in terms of gap reduction for a given generator current when the generator was a Sn-I-Sn tunnel junction. The sensor-injector junction was biased at a sufficiently high current value so that the factor S^* might be almost independent of the variation in bath temperature and its dependence could be considered as arising solely from the change in phonon transmission in superfluid helium. The phonon signal increased very rapidly with reducing bath temperature. Similar behavior was also observed for the phonons emitted from a NiCr film heater.

Figure 10 shows the measurements on the phonon signal as a function of the generator-sensor distance z at two different bath temperatures when $\Delta_s^* = \Delta_{eq}$. The results suggest that the attenuation is well approximated by an exponential function.

C. Information on spectral distribution of transmitted phonons

In order to obtain information on a phonon spectrum, we have measured the phonon signal in terms of gap reduction as a function of the sensor nonequilibrium gap $2\Delta_s^*$ utilizing a double-tunnel-junction sensor. The nonequilibrium gap was tunable from $2\Delta_{eq}$ down to $\sim 0.4\Delta_{eq}$. For $2\Delta_s^* < 0.4\Delta_{eq}$, the gap structure in the sensor-detector I-V characteristics rapidly smeared out as mentioned. The frequency range for which the spectroscopic study may be performed depends on the superconducting material used, i.e., the superconducting energy gap. For a Sn sensor, the phonons in the frequency range 120—280 GHz may be studied, whereas for a Pb sensor, those in the range 280—630 GHz may be done. Therefore the use of a combination of sensors provides a wide range of information on the phonon spectrum.

Figure 11 represents the spectroscopic data observed for the phonons emitted from a thin NiCr film heater of area 400×400 μm^2 carrying the transport current of 30 mA utilizing the Sn sensor of 200×200 μm^2. Upon reducing the sensor gap $2\Delta_s^*$, the phonon signal first decreased a little, then increased nonlinearly with a positive curvature. For $2\Delta_s^* < 0.45$ meV, the signal rapidly dropped off due to a loss of sensitivity. The observed result quite resembles the calculated one given in Fig. 4, suggesting the simple Planck distribution of phonons as expected.

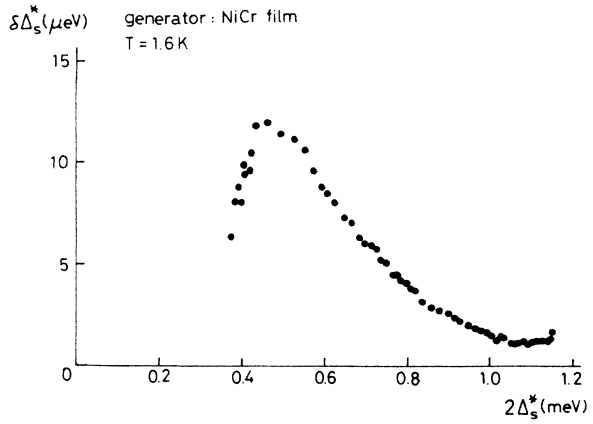

FIG. 11. Detected phonon signal in terms of sensor gap reduction as a function of the sensor nonequilibrium gap $2\Delta_s^*$ when the generator is a thin NiCr film heater.

Figure 12 shows an example of the detected phonon signal from a superconducting tunnel junction. The generator had a Sn-I-Sn-I-Sn double-tunnel-junction structure. The junction area was 300×500 μm^2 and the sensor size was 30×70 μm^2. The generator junction was biased at $V_g = 54$ mV. The phonon signal was detected at two different positions above the generator surface and both measurements yielded almost the same behavior. The rapid decrease of the signal just below $\Delta_s^* = \Delta_{eq}$ was again observable in this figure, suggesting the effect of rapid shortening of the quasiparticle recombination time as judged from Fig. 4. About $2\Delta_s^* = 0.7$ meV, corresponding to the nonequilibrium generator gap $2\Delta_g^*$; however, a qualitatively different feature from Fig. 11—a clear change in slope—was observed. The results suggest that the phenomenon cannot be interpreted solely within the picture of second sound.

D. Spatial distribution of nonequilibrium phonons

Detection of the spatial distribution of phonons was performed by moving the sample stage along the x and y axes. We have investigated the case when the generator was a thin NiCr film heater or a superconducting tunnel junction. For the latter case, the phonons emitted from the multiple-gap states of a nonequilibrium superconductor[4,5,12–15] and local inhomogeneities were detected. The sensor size was typically 20×20 μm^2 for a single-tunnel

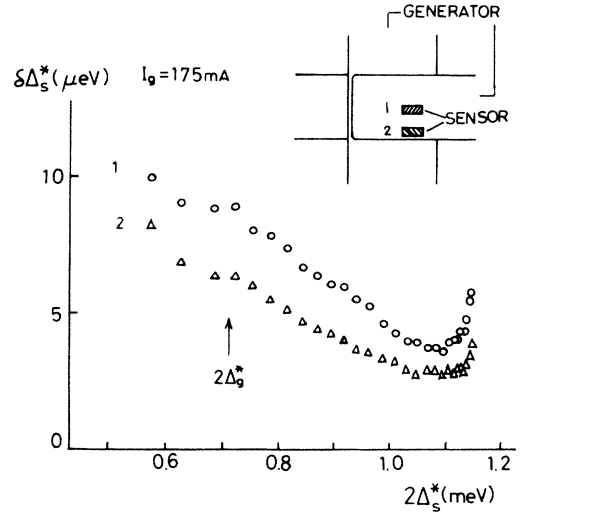

FIG. 12. Detected phonon signal in terms of sensor gap reduction as a function of the sensor nonequilibrium gap $2\Delta_s^*$ measured at two different positions when the generator is a superconducting tunnel junction.

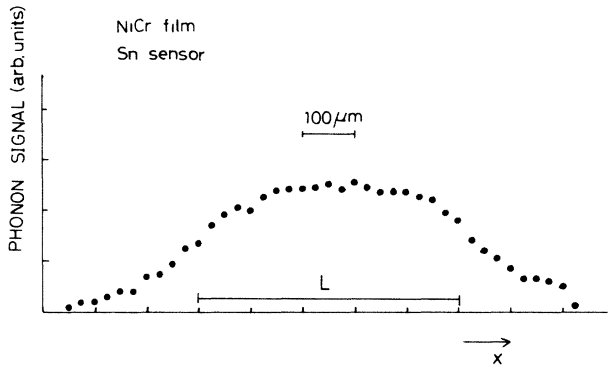

FIG. 13. Detected phonon signal in terms of sensor gap reduction as a function of position when the generator is a thin NiCr film heater.

junction and 30×60 μm^2 for a double-tunnel junction. The generator-sensor distance was around 80 μm.

When the generator was a thin NiCr film strip, the spatial distribution of the emitted phonons across the film (width: 0.5 mm), measured in terms of sensor gap reduction, was found to be quite flat, indicating the homogeneous emission of phonons from the NiCr film heater (Fig. 13).

Figure 14 shows the results for the detected phonon signal from the multiple-gap states of nonequilibrium superconducting tin films utilizing the In, Sn, and Pb sensors. The sensor gap was in its thermal equilibrium value $2\Delta_{eq}$, i.e., 1.05 meV for In, 1.15 meV for Sn, and 2.60 meV for Pb. The sensor was an S-I-N—type junction (N:Cu) in this case and the phonon signal in terms of the differential resistance at zero bias voltage was measured with and without the generator current, using a lock-in amplifier at a certain position. The net response of the phonon signal as a function of position corresponds to the data in Fig. 14. In contrast to the case of a NiCr film heater, a clear spatial structure, which was periodic, was seen for each of the sensors used. The spatial scale of an instability due to quasiparticle injection for tin was about 100 μm. This is in order-of-magnitude agreement with the calculated results.[16,17] The periodic structure was very much pronounced when a Pb sensor was used. Use of an In sensor, which means the reduction of the detectable phonon cutoff energy, yielded a relatively weak modulated structure, although the phonon signal became significantly greater. This tendency was also observed for the experiments utilizing a double-tunnel-junction sensor. When $\Delta_s^*=\Delta_{eq}$, the periodic structure was clear. On reducing the sensor gap Δ_s^* below Δ_{eq}, the phonon signal increased but the periodic modulation became relatively smaller. These facts reflect that the periodic pattern may be formed by the phonons with ultrahigh frequency ($\hbar\omega\geq2.6$ meV) which would induce an instability in a nonequilibrium system. The lower-frequency phonons would mainly contribute to form the background broad signal. By moving a sensor along both the x and y axes, we may build up the contour

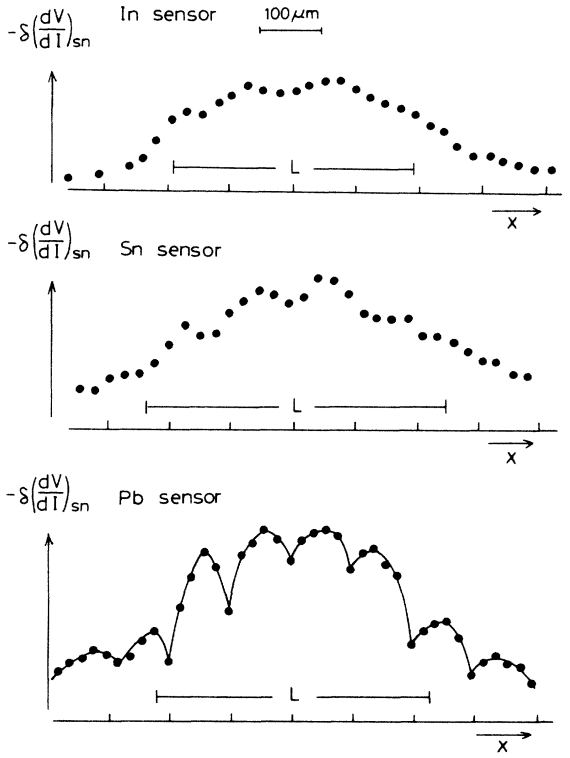

FIG. 14. Detected phonon signal in terms of the change in sensor differential resistance at zero bias voltage as a function of position for three different sensors when the generator is a superconducting tunnel junction inducing an instability by quasiparticle injection.

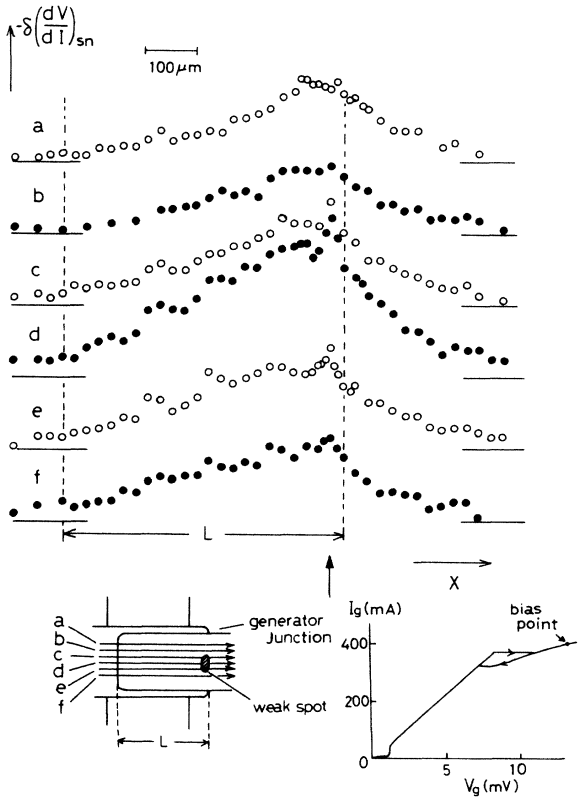

FIG. 15. Detected phonon signal in terms of the change in sensor differential resistance at zero bias voltage as a function of position when a weak spot is present in the generator junction.

map for the phonon instability structure. We found that the periodic structure was present along both the x and y axes.[5]

Finally, we show an example where there exists a weak spot in a Sn-I-Sn tunnel junction in Fig. 15. As shown in the inset, the generator I-V characteristic exhibited an hysteretic behavior in this case. Several sensor sweepings along the direction of the arrows, indicated $a-f$, were performed. We found a sharp peak in the middle part of one end of the junction. Affected by this peak, the whole phonon structure appeared rather asymmetric, indicating the influence of a heating effect which spread over the whole junction. The data suggest the existence of a weak spot in the area, shown by the hatched lines. The results also show that our phonon-detection technique could catch the localized phonons emitted from the small area, ensuring the spatial resolving power.

VI. CONCLUDING REMARKS

We finally summarize the features and limits of our new detection technique on ultrahigh-frequency phonons and discuss future aspects of it. Firstly, the method provides a high-sensitivity detection of phonons. Although the sensitivity of a superconducting tunnel sensor is the same as for the case of usual phonon spectroscopy through a solid,[1] the fraction of the transmitted phonon power from a generator to a sensor $P_{\rm det}/P_{\rm out}$ is of the order of $10^{-2}-10^{-3}$ at $T=1.7$ K when $\Delta_s^*=\Delta_{\rm eq}$ higher than the other method, because the generator-sensor separation distance can be made small. The ratio $P_{\rm det}/P_{\rm out}$ is considerably increased by lowering the phonon cutoff energy $2\Delta_s^*$ and detecting more low-frequency phonons. With a lowering of the bath temperature, both the phonon transmission in liquid helium and the sensor sensitivity are much improved. For example, for the sensor sensitivity, the phonon signal $\delta V=1$ μV, the voltage change in the excess current part of the I-V characteristic, corresponds to the incidence of phonon power of 300 μW/cm^2 at $T=1.7$ K but 10 μW/cm^2 at $T=1.0$ K. For phonon transmission, $P_{\rm det}/P_{\rm out}$ is estimated to be about 0.1 at $T=1.0$ K. Hence, the generator power 100 μW/cm^2 will yield the phonon signal of $\delta V=1$ μV at $T=1.0$ K, corresponding to detection of a phonon power of 10^{-12} W when the sensor junction of 1 μm^2 in size is used. To detect this small signal, however, it is necessary to offset the operational point by an extra phonon source such as a NiCr film heater, since the dependence of the phonon signal on generator current (or power) is strongly nonlinear, as shown in Fig. 8.

Secondly, the new phonon-detection technique provides the spectroscopic study of incident phonons by tuning the energy gap of a sensor film by quasiparticle injection utilizing a double-tunnel-junction sensor. In this work, we mainly used the tin junctions and obtained the information on a phonon spectrum in the frequency range 120–280 GHz. For a superconducting generator, a significant deviation from the thermal spectrum was obtained. To get a more sensible result, however, it is better to operate the system below $T=0.6$ K so that ballistic phonons may be transmitted dominantly. Use of different superconducting materials such as Pb, Nb, or Al provides a wide-range detection of phonon spectral information. The energy resolution is limited by the nonequilibrium gap width which is generally around $\delta\Delta_s^*/\Delta_{\rm eq}\simeq 0.04$.

Thirdly, the method provides detection of spatial distribution of phonons, provided that the gap between a generator and a sensor is made comparable to or smaller than the spatial scale of the phonon inhomogeneous distribution. In this experiment, measurements with the spatial resolution of about 20 μm were indeed attained using a sensor of 20×20 μm^2. To increase the spatial resolution, it is necessary to reduce the size of a sensor junction and to bring a generator and a sensor in closer contact as well as to improve the mechanical driving system or to introduce a new driving system. These improvements will enable us to study the phonon spatial structure with the resolution of a few μm. It is also advisable to reduce the operating temperature below $T=0.6$ K to get a sharper structure. The spatial measurements may be applied to study the nature of an instability in nonequilibrium superconductors and inhomogeneities or imperfections in tunnel junctions, metals, or semiconductors, such as GaAs, etc.

Fourthly, the response time of this method may be faster than the conventional methods of indirect detection of phonons such as the photoacoustic technique.[18,19] The response time of a sensor is, in principle, determined by the quasiparticle and phonon lifetimes of nonequilibrium superconductors. For example, it is of the order of 10 ns for Sn and of 1 ns for Pb if the phonon trapping effect is included.[8,20–22] The phonon propagation time in liquid helium is, however, around 100 ns in the case of ballistic phonons and around 1 μs in the case of second sound. Hence, the latter mainly determines the delay time.

As for the nature of the transmitted excitations through liquid helium confined to the narrow-gap region, although most of the results are consistent with the picture of second sound, a few features have not been interpreted by it. More theoretical and experimental work is needed along this line.

ACKNOWLEDGMENTS

The authors are grateful to Mr. S. Mamiya for his technical assistance. One of us (I.I.) is also grateful to Professor Y. Nannichi for helpful discussions on the phonon problem in semiconductors.

*Present address: Microelectronics Research Laboratories, NEC Corporation, 4-1-1 Miyazaki, Miyamae-ku, Kawasaki 213, Japan.

[1]See, for example, W. Eisenmenger, in *Nonequilibrium Superconductivity, Phonons and Kapitza Boundaries,* edited by K. Gray (Plenum, New York, 1981), Chap. 3, p. 73.

[2]R. C. Dynes, V. Narayanamurti, and M. Chin, Phys. Rev. Lett. **4**, 181 (1971).

[3]P. Berberich, R. Buemann, and H. Kinder, Phys. Rev. Lett. **49**, 1500 (1982).

[4]S. Kotani, Y. Suzuki, and I. Iguchi, Phys. Rev. Lett. **49**, 391 (1982).

[5]I. Iguchi and Y. Suzuki, Phys. Rev. B **28**, 4043 (1983).

[6]R. A. Sherlock, A. F. G. Wyatt, N. G. Mills, and N. A. Lockerbie, Phys. Rev. Lett. **29**, 1299 (1972).

[7]A. Rothwarf and B. N. Taylor, Phys. Rev. Lett. **19**, 27 (1967).

[8]I. Iguchi, J. Appl. Phys. **59**, 533 (1986).

[9]C. S. Owen and D. J. Scalapino, Phys. Rev. Lett. **28**, 1559 (1972).

[10]W. H. Parker, Phys. Rev. B **12**, 3667 (1975).

[11]In the case of simple heating, Δ_s^* decreases linearly with P, which is interpreted in the following way. The injected power P becomes proportional to the fourth power of the elevated temperature T^*. On the other hand, the solution of the BCS gap equation for $T^*/T_c < 0.9$ is well approximated by $\Delta_s^*/\Delta_0 = 1 - 0.695(T^*/T_c)^4$ where Δ_0 is the gap parameter at $T=0$. Hence, $(\Delta_0 - \Delta_s^*)/\Delta_0$ becomes proportional to P.

[12]I. Iguchi and D. N. Langenberg, Phys. Rev. Lett. **44**, 486 (1980).

[13]H. Akoh and K. Kajimura, Solid State Commun. **38**, 1147 (1981).

[14]I. Iguchi, S. Kotani, Y. Yamaki, Y. Suzuki, M. Manabe, and K. Harada, Phys. Rev. B **24**, 1193 (1981).

[15]I. Iguchi, in *Proceedings of the 17th International Conference on Low Temperature Physics (LT 17)*, edited by U. Eckern, A. Schmid, W. Weber, and H. Wühl (North-Holland, Amsterdam, 1984), Vol. 3, p. 165.

[16]I. Iguchi and H. Konno, Phys. Rev. B **28**, 4042 (1983).

[17]H. Konno, Prog. Theor. Phys. **69**, 674 (1983).

[18]*Optoacoustic Spectroscopy and Detection,* edited by Y. H. Pao (Academic, New York, 1977).

[19]K. Wasa, K. Tsubouchi, and N. Mikoshiba, Jpn. J. Appl. Phys. **19**, L475 (1980); **19**, L653 (1980).

[20]S. B. Kaplan, C. C. Chi, D. N. Langenberg, J.-J. Chang, S. Jafarey, and D. J. Scalapino, Phys. Rev. B **14**, 4854 (1976).

[21]P. W. Epperlein, K. Lassmann, and W. Eisenmenger, Z. Phys. B **31**, 377 (1978).

[22]I. Iguchi and A. Nishiura, J. Low Temp. Phys. **52**, 271 (1983).